Fiber Diffraction Patterns for General Unit Cells: the Cylindrically Projected Reciprocal Lattice

V. L. Finkenstadt and R. P. Millane*

Whistler Center for Carbohydrate Research and Computational Science and Engineering Program, Purdue University, West Lafayette, Indiana 47907-1160, USA. E-mail: rmillane@purdue.edu

Abstract

The positions of reflections on the diffraction pattern from a polycrystalline fiber are described by a cylindrical projection of the reciprocal lattice. The characteristics of the projection depend on the crystal system and the orientation of the fiber axis relative to the unit-cell axes. Expressions describing the cylindrically projected reciprocal lattice for a general triclinic system and any orientation of the fiber axis are derived. Calculations using these expressions illustrate characteristics of the projected reciprocal lattice and aid in the interpretation of fiber diffraction patterns.

1. Introduction

X-ray fiber diffraction analysis is used to determine the molecular and crystal structures of polymers and rod-like macromolecular assemblies that can be prepared as oriented fibers or as rotationally disordered planar arrays (Arnott, 1980; Millane, 1988). The degree of order in these specimens varies. In a *noncrystalline fiber*, the diffracting particles are oriented with their long axes approximately parallel but are randomly positioned and randomly rotated about these axes and the diffraction pattern contains continuous intensity distributed on layer lines that is equal to the cylindrical average of the intensity diffracted from a single particle. In a *polycrystalline fiber*, the molecules form small well ordered crystallites that are randomly positioned and randomly rotated about a preferred axis. The diffraction pattern consists of discrete Bragg reflections and is equivalent to the cylindrical projection of the diffraction pattern from a single crystal. Diffraction data from polycrystalline fibers have been used to determine a wide range of polynucleotide, polysaccharide and synthetic polymer structures (Arnott, 1980; Millane, 1988).

The positions of the reflections on a fiber diffraction pattern are described by the cylindrically projected reciprocal lattice (CPRL). The characteristics of the projection depend on the crystal system and the orientation of the rotation axis relative to the unit-cell axes. Because of the cylindrical projection, determination of the unit-cell dimensions from a fiber diffraction pattern is not necessarily straightforward or even unambiguous.

Many biopolymers in polycrystalline fibers crystallize in a monoclinic (or orthorhombic or hexagonal) system where the monoclinic angle is in a plane that is normal to the rotation axis. Although difficulties can arise because of reflection overlap in projection, interpretation of the diffraction pattern in terms of the cell constants is usually straightforward. However, if the cell is triclinic or the rotation axis is not coincident with one of the unit-cell axes, then interpretation of the projected reciprocal lattice may not be so easy. We derive here expressions describing the cylindrically projected reciprocal lattice for the general case of a triclinic system and any orientation of the rotation axis, and use them to illustrate characteristics of the projected reciprocal lattice. The results should be useful in the interpretation of fiber diffraction patterns.

2. Preliminaries

We define cylindrical polar coordinate systems (r, φ, z) and (R, ψ, Z) in real and reciprocal space, respectively, with the z and Z axes parallel. The specimen consists of crystallites that are randomly positioned, and oriented such that the lines, denoted by ℓ, that have a fixed orientation relative to the unit-cell axes in each crystallite are all parallel (Fig. 1a). The crystallites are randomly rotated about ℓ. The z axis is chosen to be parallel to ℓ so that the reciprocal lattice is cylindrically projected about the Z axis (the rotation or fiber axis). The crystallites diffract independently and, as a result of their random rotations, the measured intensity is the cylindrical average of the intensity diffracted by a representative crystallite. The intensity on a fiber diffraction pattern therefore consists of sharp reflections positioned on the CPRL, denoted by $\mathcal{L}(R, Z)$, given by

$$\mathcal{L}(R, Z) = \int_0^{2\pi} L(R, \psi, Z)\, d\psi, \tag{1}$$

where $L(R, \psi, Z)$ denotes the reciprocal lattice expressed as a function of polar coordinates. The CPRL can therefore be written as

$$\mathcal{L}(R, Z) = \sum_{h,k,l} \delta(R - R(h, k, l), Z - Z(h, k, l)), \tag{2}$$

where $\delta(\,)$ is the Dirac delta function and $R(h, k, l)$ and $Z(h, k, l)$ are the cylindrical polar coordinates of the reciprocal-lattice point (h, k, l). The CPRL is therefore described by the functions $R(h, k, l)$ and $Z(h, k, l)$, which depend, of course, on the cell constants and the orientation of the line ℓ. The spherical polar radius of the reflection hkl, $\rho(h, k, l)$, is given by

$$\rho^2(h, k, l) = h^2 a^{*2} + k^2 b^{*2} + l^2 c^{*2} + 2hka^* b^* \cos \gamma^*$$
$$+ 2hla^* c^* \cos \beta^* + 2klb^* c^* \cos \alpha^* \quad (3)$$

and is related to $R(h, k, l)$ and $Z(h, k, l)$ by

$$\rho^2(h, k, l) = R^2(h, k, l) + Z^2(h, k, l). \quad (4)$$

In a polycrystalline fiber specimen, the crystallites are generally randomly oriented 'up and down'. If c is parallel to the fiber axis, then the crystallites are randomly rotated by 0 or 180° about an axis normal to c or the Z axis. If c is not parallel to the fiber axis, we assume (as is probable) that the crystallites are randomly rotated by 0 or 180° about an axis normal to the fiber axis. In either case, for every reciprocal-lattice point (h, k, l), there is another $(\bar{h}, \bar{k}, l)$ for which $R(\bar{h}, \bar{k}, l) = R(h, k, l)$ and $Z(\bar{h}, \bar{k}, l) = -Z(h, k, l)$ so that the rotation has no effect on the cylindrical projection and one need consider only, say, positive values of Z.

3. The cylindrically projected reciprocal lattice

It is convenient to consider two cases separately; the first where the rotation axis ℓ is parallel to one of the unit-cell axes and the second where it is not.

3.1. Rotation about a unit-cell axis

The molecules in a fiber specimen are usually periodic and the molecular axes are parallel to one of the unit-cell axes. Furthermore, the molecular axes usually define the axis of rotation so that the rotation is normally about a unit-cell axis, which is taken here to be c, i.e. c is parallel to the z axis. This leads to simplifications because, since a^* and b^* are always perpendicular to c, the $a^* b^*$ plane, or the hk net, is normal to the Z axis. Therefore, reflections for a fixed l lie on layer lines that are parallel to the R axis and are separated by $\Delta Z = 1/c$, irrespective of the unit-cell angles, so that

$$Z(h, k, l) = l/c. \quad (5)$$

The most common crystal systems encountered in polycrystalline fibers are orthorhombic, hexagonal (with $\gamma = 120°$) or monoclinic (with $\gamma \neq 90°$). In these cases, since $\alpha^* = \beta^* = 90°$, c^* is parallel to c and the Z axis, and the reciprocal lattice is cylindrically projected about c^*. Reference to (3), (4) and (5) shows that

$$R^2(h, k, l) = h^2 a^{*2} + k^2 b^{*2} + 2hka^* b^* \cos \gamma^*. \quad (6)$$

Since $R(h, k, l)$ is independent of l, and therefore Z, reflections of fixed h and k form straight row lines that are parallel to the Z axis. Since the row lines are parallel, interpretation of the CPRL is usually straightforward, difficulties arising only if different row lines overlap in an ambiguous manner.

If the crystal system is either triclinic or monoclinic with α^* or β^* the monoclinic angle, then c^* is not parallel to the Z axis and the cylindrical projection is not about c^*.
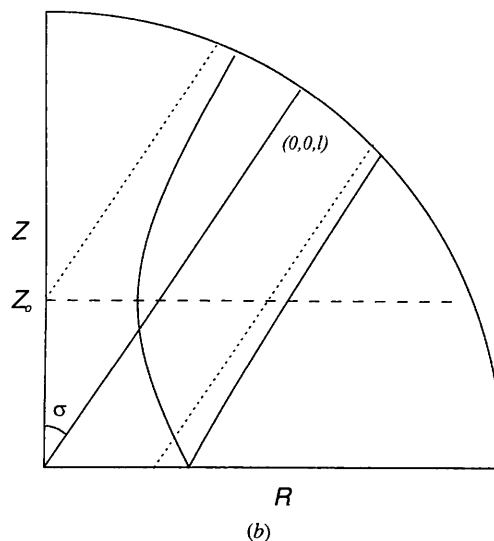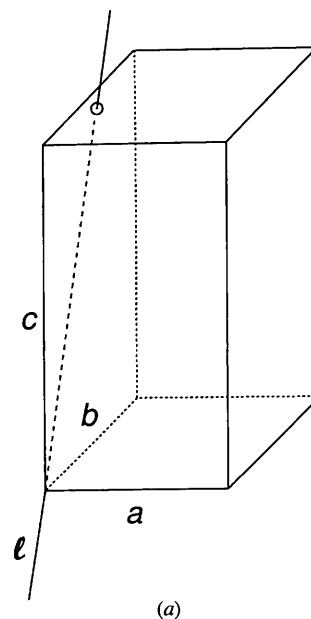

(a)

(b)

Fig. 1. (a) Illustration of the fiber, or rotation, axis (ℓ) relative to the unit cell. (b) Illustration of a hyperbolic row line (solid line) for an untilted triclinic system, shown in one quadrant of the cylindrically projected reciprocal space. The $(0, 0, l)$ row line (solid line through the origin) and the asymptotes (dotted lines) for the row lines are also shown. The dashed line shows the focal axis.

Using (3), (4) and (5) shows that $R(h, k, l)$ is then given by

$$R^2(h, k, l) = h^2 a^{*2} + k^2 b^{*2} + l^2(c^{*2} - 1/c^2)$$
$$+ 2hka^* b^* \cos \gamma^* + 2hla^* c^* \cos \beta^*$$
$$+ 2klb^* c^* \cos \alpha^*. \qquad (7)$$

Setting $l = Zc$ allows (7) to be put in the form

$$R^2/A^2 - (Z - Z_o)^2/B^2 = 1, \qquad (8)$$

where the constants A, B and Z_o (derived in Appendix A) depend only on h, k and the cell constants. Equation (8) is the equation of the row lines, parameterized by h and k, which are therefore hyperbolae with focus on the Z axis at $Z = Z_o$ and focal axis parallel to the R axis. This is illustrated in Fig. 1(b), which shows one quadrant of the projected reciprocal space. Substituting $h = k = 0$ in (7) shows that the equation of the $(0, 0, l)$ row line is given by

$$Z = (c^2 c^{*2} - 1)^{-1/2} R. \qquad (9)$$

The $(0, 0, l)$ row line is therefore always a straight line through the origin of reciprocal space (Fig. 1b). Noting that the angle σ between $\mathbf{c}$ and $\mathbf{c}^*$ is given by $\cos \sigma = 1/(cc^*)$, (9) may be written as

$$Z = \cot \sigma R. \qquad (10)$$

The asymptotes for the hyperbolae are parallel to the $(0, 0, l)$ row line, pass through the focus (Fig. 1b) and are given by

$$Z = \cot \sigma R \pm Z_o, \qquad (11)$$

where (see Appendix A)

$$Z_o = [cc^*(ha^* \cos \beta^* + kb^* \cos \alpha^*)]/(1 - c^2 c^{*2}). \qquad (12)$$

As a result of the presence of up and down crystallites, each hyperbola is reflected in the R axis so that each row line consists of segments of two hyperbolae with focal axes at $Z = \pm Z_o$ and the two asymptotes given by (11) as shown in Fig. 1(b).

3.2. Rotation axis inclined to the unit-cell axes

Although in most fiber specimens the crystallites are aligned with one of the unit-cell axes (generally corresponding to the molecular axis) parallel to the rotation axis, in some cases the rotation axis may be inclined at a (usually small) angle to the unit-cell axis. The fiber is then often referred to as being *tilted*, examples being some polyesters (Daubeny et al., 1954; Hall, 1984; Fu et al., 1994), collagen (Fraser & MacRae, 1981; Fraser et al., 1983; Wess et al., 1995) and fd *Inovirus* (Welsh et al., 1996). A good example of a tilted polycrystalline fiber system is collagen, for which a typical diffraction pattern (courtesy of T. Wess) is shown

in Fig. 2. The collagen unit cell and its orientation relative to the fiber axis have been studied in detail by Fraser & MacRae (1981).

In a tilted specimen, the Z axis is not normal to the $a^* b^*$ plane so that (5) is not satisfied and $Z(h, k, l)$ depends in general on h, k and l. However, since the angle between $\mathbf{c}$ and the Z axis, which we refer to as the tilt and denote by τ, is usually small (i.e. a few degrees), it is convenient to think of the projected reciprocal-lattice points as being shifted by a small amount from the positions they would occupy if the crystallites were not tilted to the rotation axis. It is convenient to describe the tilt in reciprocal space. From Fig. 3(a), $\mathbf{c}$ is rotated by τ relative to the Z axis, about the line m that passes through the origin of reciprocal space, lies in the plane normal to the Z axis and makes an angle θ with $\mathbf{a}^*$. Since the tilt is the same in real and reciprocal spaces, the direction of the line ℓ (Fig. 1a) is obtained by rotating $\mathbf{c}$ by $-\tau$ about m. Inspection of Fig. 3(a) shows that, on the $l = 0$ reciprocal-lattice plane, the distance x_o of a reciprocal-lattice point $(h, k, 0)$ from the line m is

$$x_o = ha^* \sin \theta - kb^* \sin(\gamma^* - \theta). \qquad (13)$$

The reciprocal-space coordinates (ξ, η) of the projection of the origin of the lth layer plane onto the zero layer are given by

$$\xi = lc^*(\cos \alpha^* - \cos \beta^* \cos \gamma^*)/\sin^2 \gamma^* \qquad (14)$$

and

$$\eta = lc^*(\cos \beta^* - \cos \alpha^* \cos \gamma^*)/\sin^2 \gamma^*. \qquad (15)$$

Therefore, the distance x of the projection Q' of a general reciprocal-lattice point $Q(h, k, l)$ onto the zero layer from
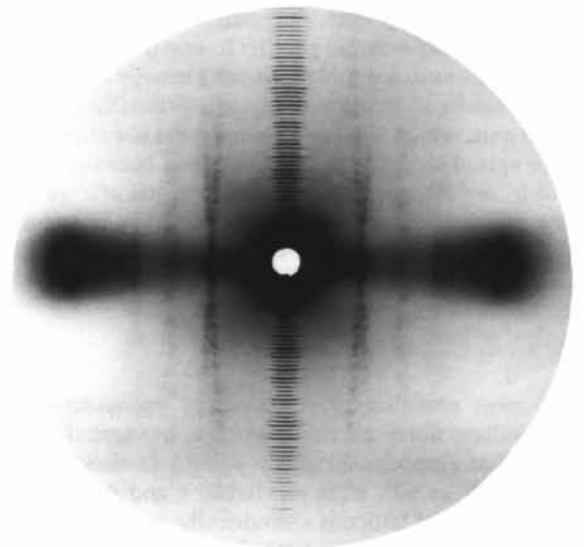

Fig. 2. Fiber diffraction pattern from stained type I tendon collagen (Wess et al., 1995) showing fanning of the row lines.

the line m is

$$x = (ha^* + \xi)\sin\theta - (kb^* + \eta)\sin(\gamma^* - \theta). \qquad (16)$$

Reference to Fig. 3(b) shows that the distance of Q from the equatorial plane, $Z(h, k, l)$, is

$$Z(h, k, l) = (l\cos\tau/c) - x\sin\tau, \qquad (17)$$

so that

$$Z(h, k, l) = (l\cos\tau/c) + [(kb^* + \eta)\sin(\gamma^* - \theta)$$
$$- (ha^* + \xi)\sin\theta]\sin\tau. \qquad (18)$$

Equation (18) gives the Z coordinates of the CPRL points and the radial coordinates, $R(h, k, l)$, are obtained by substituting (3) and (18) into (4). The resulting equations for the row lines are very complicated. The concept of a single layer line does not apply for a tilted system since, for a particular l, reflections hkl lie on a variety of curves that depend on the values of h and k. One can think of 'layer lines' for fixed h, say, and l, and variable k, however. To avoid confusion, we refer to these as 'pseudo layer lines'. For example, reflections for which $h = 1$ and $l = 2$ lie on the $(1, k, 2)$ pseudo layer line. For small values of the tilt, the reciprocal-lattice points are rotated by a small angle, between $-\tau$ and τ, about the origin of the fiber diffraction pattern, from their positions at zero tilt. Reflections that overlap for an untilted specimen separate into distinct reflections. This can aid in the indexing of reflections.

The diffraction pattern from collagen (Fig. 2) clearly shows 'fanning' of the row lines, particularly about the meridian and on the first group of row lines from the meridian. The fanning is due to a combination of both a triclinic unit cell and tilting of the crystallites. The angular extent of the fanning is small since α and β deviate by less than $5°$ from $90°$ and the tilt is small ($\sim 2°$). Fanning of the layer lines is not easily observed because of the large c repeat.

For a triclinic system there is a particular tilt (*i.e.* specific values of τ and θ) that puts the ab plane normal to the rotation axis. In this case, c^* is parallel to the Z axis and the reciprocal lattice is rotated about c^*. The (h, k) row lines are then straight lines parallel to the Z axis, as in the case of an untilted monoclinic system, but there are not single layer lines for a fixed l. The reflections that lie on hyperbolic row lines for the untilted triclinic system are rotated about the center of the pattern such that they move off the original layer lines but onto straight row lines. The particular values of τ and θ required can be calculated as follows. Since for an untilted system c is coincident with the z axis, for the above conditions to apply c^* must be rotated onto the position originally occupied by c. The crystallites must therefore be rotated about the line m with direction $c \times c^*$, which makes an angle θ to a^* given by

$$\cos\theta = a^* \cdot (c \times c^*)/(a^*|c \times c^*|). \qquad (19)$$

The rotation τ is the angle between c and c^*, *i.e.*

$$\cos\tau = \cos\sigma = 1/(cc^*). \qquad (20)$$

The required tilt can be calculated from the unit-cell constants using (19) and (20). This kind of tilt was considered by Welsh *et al.* (1996), who termed it 'type II tilt', in their analysis of the fiber diffraction patterns from fd *Inovirus*, although they concluded that this kind of tilt was not present.
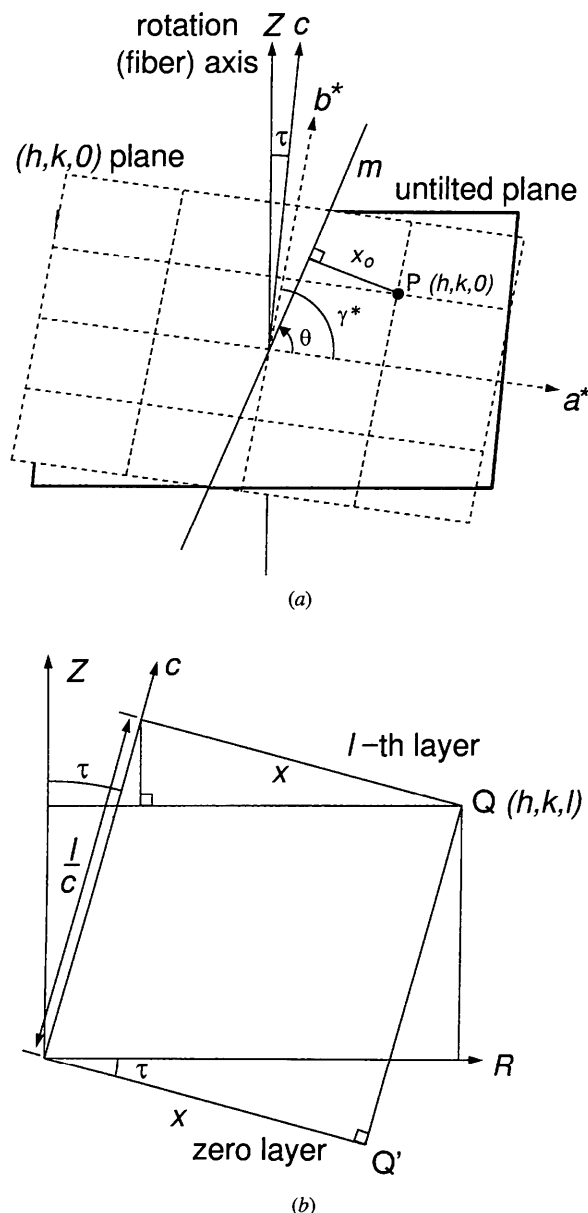

Fig. 3. (*a*) The equatorial (untilted) plane and the $(h, k, 0)$ plane in reciprocal space for a tilted fiber (refer to the text). (*b*) Projection along the rotation line m in reciprocal space showing projections of the zeroth and lth layer planes (refer to the text).

The crystallites in a real polycrystalline fiber are subject to disorientation, *i.e.* the lines ℓ for each crystallite are not exactly parallel but are distributed over a small angle relative to their average direction (the fiber axis). The effect of disorientation is to smear each reciprocal-lattice point into an arc, centered on the origin of the fiber diffraction pattern. Hence distinct reflections for tilted specimens will be observed only if the mean disorientation is less than the tilt. However, as long as the disorientation is not too large, tilt is evidenced by splitting of the arcs. The maximum angular spread of a set of reflections is equal to the sum of the effects of disorientation and tilt. If the disorientation is small or can be estimated, the tilt angle can be estimated by measuring the maximum angular spread of the reflections (Welsh *et al.*, 1996). The orientation θ of the tilt axis can be estimated by examining the distribution of the deviations of the positions of the reflections from their positions in an untilted fiber (Daubeny *et al.*, 1954). The parameters τ and θ can be refined by least-squares fitting between the measured and calculated reflection positions (Fraser *et al.*, 1983).
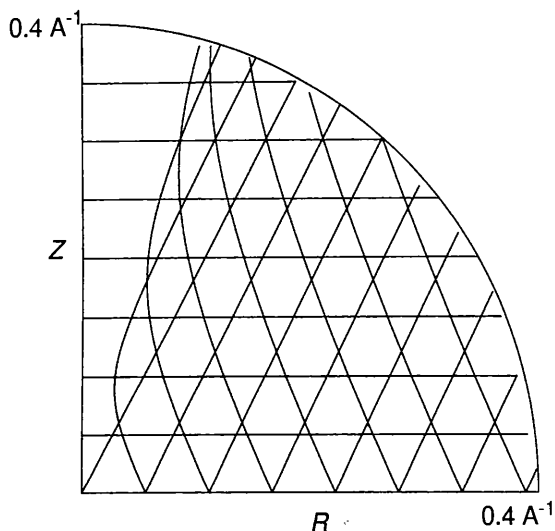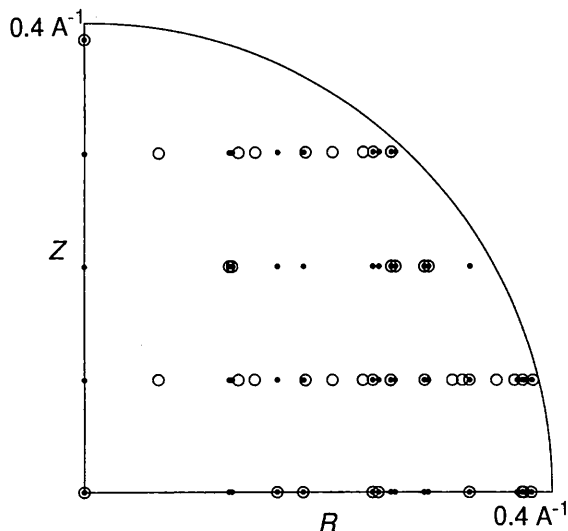

Fig. 4. Layer lines and $(0, k)$ row lines for an untilted triclinic unit cell with $b = c = 20$ Å, $\alpha = 70$, $\beta = 75$ and $\gamma = 100°$.
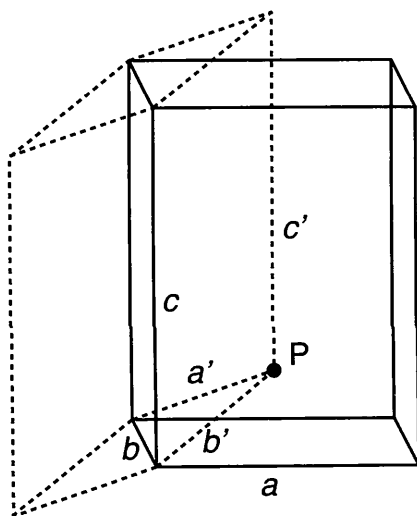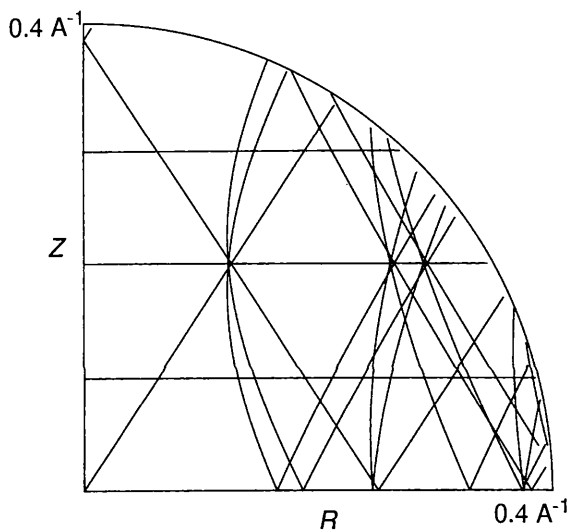

(a)

Fig. 5. Relationship between the monoclinic unit cell for cellulose Iβ (solid lines) and the triclinic unit cell for cellulose Iα' (dashed lines). The point P has fractional coordinates $(\frac{1}{2}, \frac{1}{2}, \frac{1}{4})$ in the monoclinic system.

(b)

Fig. 6. (a) CPRL points for triclinic cellulose Iα' (open circles) and monoclinic cellulose Iβ (filled circles). (b) Row lines and layer lines for triclinic cellulose Iα'.

4. Examples

We show here some examples of the CPRL. These are presented either as projected reciprocal-lattice points or as plots of certain row lines and layer lines (or pseudo layer lines) in Figs. 4–8. The intersections between row lines and layer lines represent projected reciprocal-lattice points. However, only intersections between row lines and pseudo layer lines that have common values of h and k represent projected reciprocal-lattice points. Note that because a flat detector, for example, records a slightly distorted form of the projected reciprocal lattice, Figs. 4–8 correspond approximately, but not exactly, to what would be seen on an actual recorded fiber diffraction pattern.

For an untilted monoclinic unit cell ($\gamma \neq 90°$), the row lines of constant h and k are straight lines parallel to the Z

Table 1. *Unit-cell dimensions for cellulose I*

	a (Å)	b (Å)	c (Å)	α (°)	β (°)	γ (°)
Cellulose Iβ	8.00	8.17	10.36	90.00	90.00	97.30
Cellulose Iα	5.93	6.74	10.36	113.00	117.00	81.00
Cellulose Iα'	5.94	6.60	10.36	113.10	115.85	81.11

axis. For an untilted triclinic unit cell, $\mathbf{c}^*$ is inclined to the Z axis and the row lines form hyperbolae as described in §3.1. This is illustrated in Fig. 4, which shows the layer lines and $(0, k)$ row lines for a triclinic unit cell.

Cellulose I forms crystalline fibers and often exists as a mixture of two crystalline allomorphs, referred to as cellulose Iα and Iβ, which are triclinic and monoclinic (Table 1), respectively (Sugiyama *et al.*, 1991). The two unit cells are closely related and we use them here to
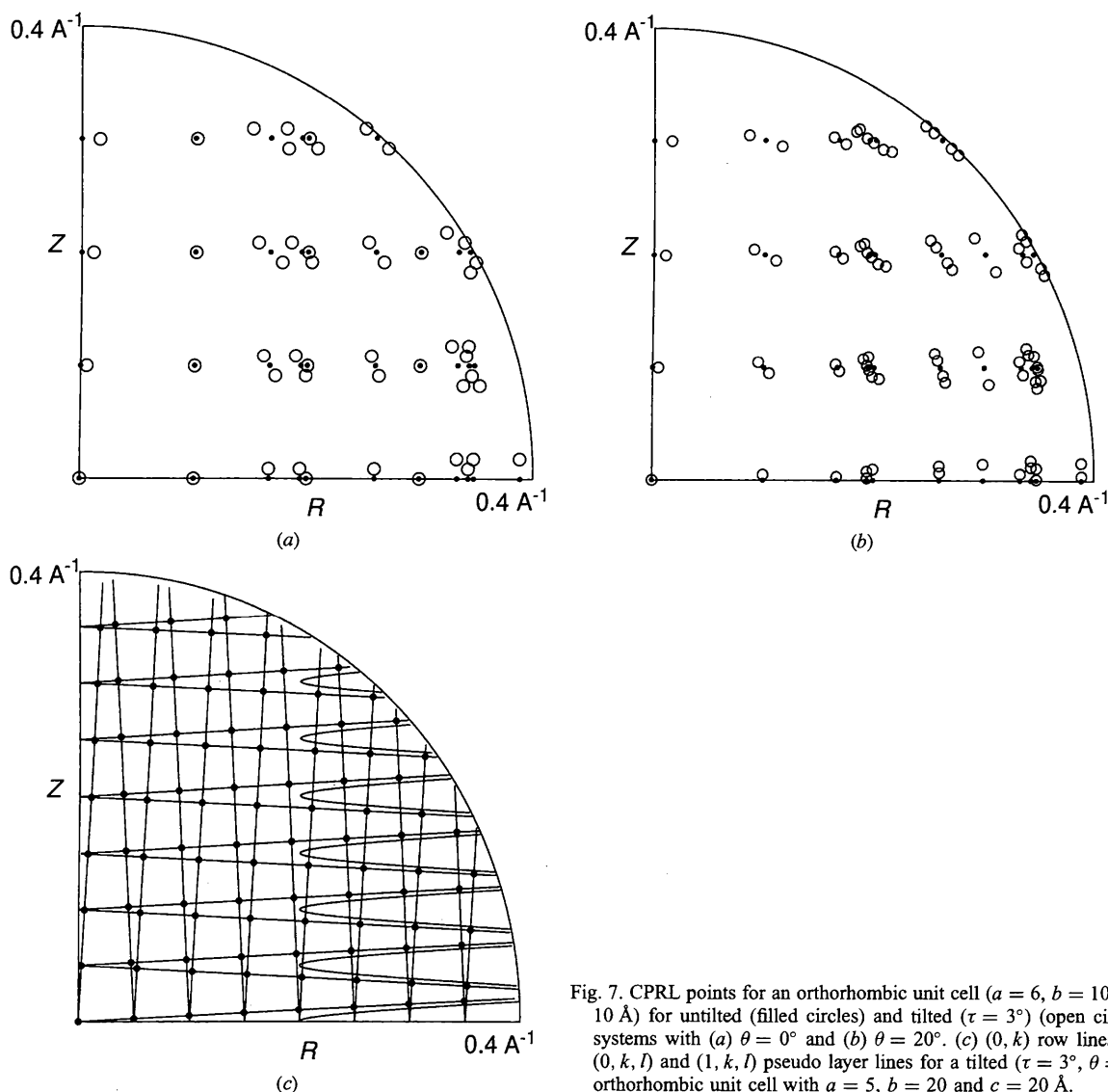

(a)

(b)

(c)

Fig. 7. CPRL points for an orthorhombic unit cell ($a = 6$, $b = 10$, $c = 10$ Å) for untilted (filled circles) and tilted ($\tau = 3°$) (open circles) systems with (a) $\theta = 0°$ and (b) $\theta = 20°$. (c) $(0, k)$ row lines and $(0, k, l)$ and $(1, k, l)$ pseudo layer lines for a tilted ($\tau = 3°$, $\theta = 0°$) orthorhombic unit cell with $a = 5$, $b = 20$ and $c = 20$ Å.

illustrate the CPRL for untilted triclinic and monoclinic systems. The unit-cell vectors $\mathbf{a}'$, $\mathbf{b}'$ and $\mathbf{c}'$ for the triclinic cell are approximately related to those of the monoclinic unit cell, $\mathbf{a}$, $\mathbf{b}$ and $\mathbf{c}$, by

$$\mathbf{a}' = -\mathbf{a}/2 + \mathbf{b}/2 - \mathbf{c}/4$$
$$\mathbf{b}' = -\mathbf{a}/2 - \mathbf{b}/2 - \mathbf{c}/4 \tag{21}$$
$$\mathbf{c}' = \mathbf{c}$$

(Fig. 5). For purposes of comparison of the CPRL for the monoclinic and triclinic cells, we adjust the cell constants of the triclinic unit cell so that (21) is satisfied *exactly* and refer to the triclinic unit cell as cellulose Iα' (Table 1). The volume of the triclinic unit cell is half that of the monoclinic unit cell and the triclinic unit-cell vectors are

related to those for the monoclinic unit cell by

$$\mathbf{a}'^* = -\mathbf{a}^* + \mathbf{b}^*$$
$$\mathbf{b}'^* = -\mathbf{a}^* - \mathbf{b}^* \tag{22}$$
$$\mathbf{c}'^* = \mathbf{c}^* - \mathbf{a}^*/2.$$

Fig. 6(a) shows the CPRL for cellulose Iα and Iβ as open and filled circles, respectively. The reflections for the monoclinic unit cell are seen to lie on vertical row lines whereas those for the triclinic unit cell do not. Because of the relationships between the two unit cells, certain reciprocal-lattice points for the two cells coincide and therefore coincide on the CPRL. Using (22) shows that this occurs when the following conditions between the indices for the monoclinic (h, k, l) and triclinic (h', k', l')
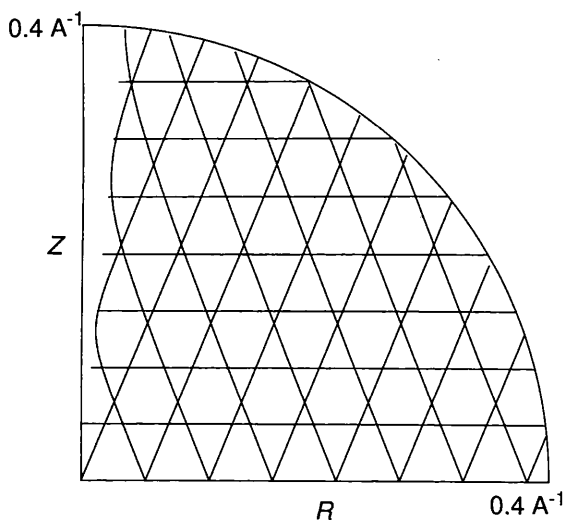
(a)
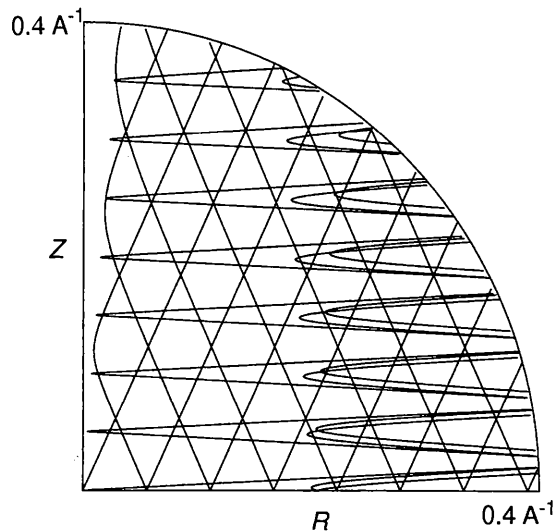
(b)
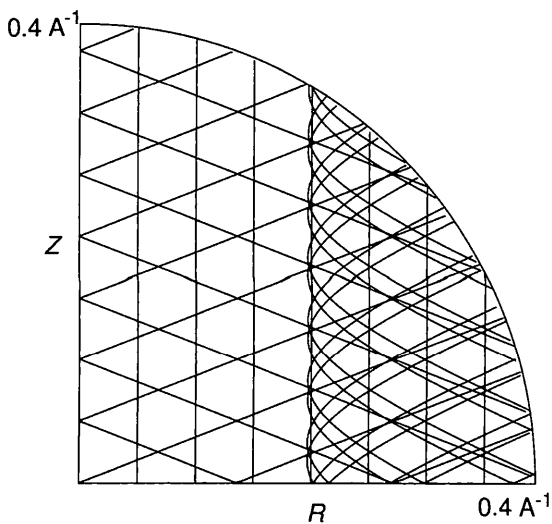
(c)

Fig. 8. $(0, k)$ row lines and $(0, k, l)$ and $(\pm 1, k, l)$ pseudo layer lines for a triclinic system ($a = 5$, $b = 20$, $c = 20$ Å, $\alpha = 70$, $\beta = 85$, $\gamma = 100°$) for (a) no tilt ($\tau = 0°$), (b) tilted ($\tau = 3°$, $\theta = 0°$), and (c) tilted ($\tau = -21.9°$, $\theta = -25.1°$) such that the ab plane is normal to the fiber axis.

cells are satisfied:

$$h = -h' - k' - l'/2$$
$$k = h' - k' \qquad (23)$$
$$l = l'.$$

These equations can only be satisfied on the even layer lines and give rise to some of the coincidences seen in Fig. 6(a). Other coincidences may also occur where reflections have the same (R, Z) coordinates as seen for some reflections on the odd layer lines in Fig. 6(a). All of the row lines and layer lines for the triclinic unit cell are shown in Fig. 6(b). The row lines are seen to form a complex system of hyperbolae.

The effects of $\mathbf{c}$ being tilted to the rotation axis for an orthorhombic system are shown in Fig. 7. The CPRL for rotation about $\mathbf{a}^*$ ($\theta = 0°$) and about a line inclined to $\mathbf{a}^*$ ($\theta = 20°$) are shown in Figs. 7(a) and (b), respectively. Coincident reflections for an untilted fiber (filled circles) are rotated about the origin of the diffraction pattern, splitting into sets of distinct reflections shown by the open circles for a tilted fiber. Some reflections remain coincident when the rotation axis coincides with the reciprocal-cell axis (Fig. 7a), whereas they split when the rotation axis is inclined to the unit-cell axes (Fig. 7b). Some of the row lines and pseudo layer lines for a tilted orthorhombic system ($\theta = 0°$) are shown in Fig. 7(c). Each row line for an untilted system splits into two row lines (as a result of reflection in the R axis), the $(0, k)$ row lines being shown in Fig. 7(c). Each layer line splits into many pseudo layer lines, those for $h = 0$ and 1 being shown in Fig. 7(c). The intersections between row lines and pseudo layer lines that correspond to projected reciprocal-lattice points are shown by filled circles in Fig. 7(c).

The effect of tilting a triclinic system is shown in Fig. 8. The $(0, k)$ row lines and the $(0, k, l)$ and $(\pm 1, k, l)$ pseudo layer lines for an untilted system are shown in Fig. 8(a). The same row lines and layer lines for a tilt of 3° are shown in Fig. 8(b). The hyperbolic row lines change positions, and the overlapping pseudo layer lines split into three distinct curves. The effect of the crystallites being tilted such that the ab plane is normal to the fiber axis is shown in Fig. 8(c). The hyperbolic row lines for the untilted system (Fig. 8a) reduce to straight lines parallel to the Z axis (Fig. 8c). As a result of the larger tilt, the pseudo layer lines are now more spread out and overlap (Fig. 8c).

5. Conclusions

The positions of the reflections on a diffraction pattern from a polycrystalline fiber are described by the cylindrically projected reciprocal lattice. Although monoclinic (or orthorhombic or hexagonal) crystal systems are most common with polymers, triclinic systems are not uncommon. In most fibers, the molecular axes, or the crystallite c axes, are parallel to the fiber axis. The layer lines are then parallel to the R axis. For a monoclinic system, the row lines are parallel to the Z axis whereas, for a triclinic system, the row lines form hyperbolae. In some cases, the c axes are tilted by a small angle to the fiber axis, in which case the cylindrically projected reciprocal lattice is more complicated. There are no longer layer lines as for an untilted fiber, but the layer lines split into curves, one for each value of h (or k). Reflections in the pattern from a tilted fiber are rotated from the positions they would have in the diffraction pattern from an untilted fiber. This splitting can aid in structure determination (Daubeny et al., 1954). The precise structural basis for tilting has not been determined in cases where it is observed (Daubeny et al., 1954; Fraser et al., 1983; Hall, 1984; Welsh et al., 1996). However, since it is usually very precise, it presumably results from preferred specific interactions between the molecules in different crystallites. There is a particular tilt (magnitude and direction) for a triclinic system that brings the ab plane normal to the fiber axis, in which case the diffraction pattern has straight row lines parallel to the Z axis. Expressions have been derived here that allow the cylindrically projected reciprocal lattice to be calculated for any tilted triclinic system. These allow one to explore the characteristics of the projected reciprocal lattice, and aid in the interpretation of fiber diffraction patterns.

APPENDIX A
Equations of the row lines for untilted fibers

Equation (7) with $Z = lc$ for the row lines can be put in the form

$$R^2 = DZ^2 + EZ + F, \qquad (24)$$

where

$$D = c^2 c^{*2} - 1, \qquad (25)$$

$$E = 2cc^*(ha^* \cos \beta^* + kb^* \cos \alpha^*) \qquad (26)$$

and

$$F = h^2 a^{*2} + k^2 b^{*2} + 2hka^* b^* \cos \gamma^*. \qquad (27)$$

Equation (24) can be written in the form for a hyperbola (8) as

$$R^2/A^2 - (Z - Z_o)^2/B^2 = 1, \qquad (28)$$

where

$$A^2 = (4DF - E^2)/4D, \qquad (29)$$

$$B^2 = (4DF - E^2)/4D^2 \qquad (30)$$

and

$$Z_o = -E/2D. \tag{31}$$

Substituting from the above equations allows equation (12) for the Z coordinate of the focus (Z_o) to be derived. The equation of the asymptotes is

$$Z = (B/A)R + Z_o = D^{-1/2}R + Z_o, \tag{32}$$

and substituting from the above gives equation (11) for the asymptotes.

References

Arnott, S. (1980). *Fiber Diffraction Methods*, edited by A. D. French & K. H. Gardner, pp. 1–30. *Am. Chem. Soc. Symp. Ser.* Vol. 141. Washington: American Chemical Society.

Daubeny, R. P., Bunn, C. W. & Brown, C. J. (1954). *Proc. R. Soc. London Ser. A*, **226**, 531–542.

Fraser, R. B. D. & MacRae, T. P. (1981). *Int. J. Biol. Macromol.* **3**, 193–200.

Fraser, R. B. D., MacRae, T. P., Miller, A. & Suzuki, E. (1983). *J. Mol. Biol.* **167**, 497–521.

Fu, Y., Annis, B., Boller, A., Jin, Y. & Wunderlich, B. (1994). *J. Polym. Sci. Polym. Phys. Ed.* **32**, 2289–2306.

Hall, I. H. (1984). *Structure of Crystalline Polymers*, edited by I. H. Hall, pp. 39–77. New York: Elsevier Applied Science Publishers.

Millane, R. P. (1988). *Computing in Crystallography 4: Techniques and New Technologies*, edited by N. W. Isaacs & M. R. Taylor, pp. 169–186. Oxford University Press.

Sugiyama, J., Young, R. & Chanzy, H. (1991). *Macromolecules*, **24**, 4168–4175.

Welsh, L. C., Symmons, M. F., Nave, C., Perham, R. N., Marseglia, E. A. & Marvin, D. A. (1996). *Macromolecules*, **29**, 7075–7083.

Wess, T. J., Hammersley, A., Wess, L. & Miller, A. (1995). *J. Mol. Biol.* **248**, 487–493.